

# Density of states in a superconductor carrying a supercurrent

A. Anthore, H. Pothier, and D. Esteve

*Service de Physique de l'Etat Condensé, Direction des Sciences  
de la Matière, CEA-Saclay, 91191 Gif-sur-Yvette, France*

(Dated: November 19, 2018)

We have measured the tunneling density of states (DOS) in a superconductor carrying a supercurrent or exposed to an external magnetic field. The pair correlations are weakened by the supercurrent, leading to a modification of the DOS and to a reduction of the gap. As predicted by the theory of superconductivity in diffusive metals, we find that this effect is similar to that of an external magnetic field.

PACS numbers: PACS numbers: 74.78.Na, 74.20.Fg, 74.25.Sv

How is the superconducting order modified by a supercurrent? The superconducting order is based on pairing electronic states which transform into one another by time reversal [1]. The ground-state wavefunction corresponds to a coherent superposition of doubly empty and doubly occupied time-reversed states, in an energy range around the Fermi level given by the BCS gap energy. When an external magnetic field  $\vec{B} = \text{curl } \vec{A}$  is applied, time-reversed states are dephased differently, resulting in a weakening of superconductivity. In presence of a supercurrent, the superconducting order no longer corresponds to the pairing of time-reversed states, which results in a kinetic energy cost, and again in a weakening of superconductivity. In the early stages of the theory of superconductivity, it was found that, in diffusive superconductors (in which the electron mean-free-path is short compared to the BCS coherence length) and in homogeneous situations, the modification of the superconducting order by a magnetic field, by a current and by paramagnetic impurities could be described by a single parameter, the depairing energy  $\Gamma$  [2]. Later on, the reformulation of the theory by Usadel [3, 4] in the diffusive limit extended this equivalence to inhomogeneous situations, where the modulus of the order parameter may vary in space. In the Usadel equations, all physical quantities only involve the intrinsic combination  $\vec{\nabla}\varphi - (2e/\hbar)\vec{A}$ , where the gradient  $\vec{\nabla}\varphi$  in the phase of the superconducting order parameter is associated with the supercurrent, revealing the equivalence of a supercurrent and of an applied magnetic field. The Usadel equations are now at the basis of the understanding of mesoscopic superconductivity in diffusive conductors [5, 6]. Experimentally, measurements of the density of states (DOS) in a thin superconductor placed in an in-plane magnetic field were well accounted for by the concept of depairing energy [7]. In contrast, the effect of a supercurrent has been partly addressed in a single experiment, focused on the reduction of the superconducting gap close to the critical temperature [8]. A complication of the experiments with a supercurrent is that, if the sample width exceeds the London penetration length  $\lambda_L$ , the current distribution given by the non-local equations of electrodynamics [9] is

not homogeneous. In the experiment reported here, the superconductor is wire-shaped, with thickness and width smaller than  $\lambda_L$ , so that the current flow is homogeneous and the magnetic field penetrates completely. Moreover, the effect of the magnetic field induced by the supercurrent is then negligible. This simple geometry allows to test the fundamental equivalence between the effect of a magnetic field and of a supercurrent in a diffusive superconductor, and to compare precisely with the predictions of the Usadel equations.

Our experiment was performed on a current-biased superconducting wire made of aluminum, placed in a perpendicular magnetic field  $B$  (see Fig. 1). The density of states in the wire was inferred from the differential conductance  $dI/dV(V)$  of a tunnel junction formed between a small section of the wire and a normal probe electrode made of copper. Disregarding Coulomb blockade and temperature effects (see below),  $dI/dV(V)$  is proportional to the DOS  $n(eV)$ . The sample was fabricated in an electron-beam evaporator in a single pump-down, using three-angle shadow-mask technique through a PMMA suspended mask patterned using e-beam lithography [10]. The substrate was thermally oxidized silicon.

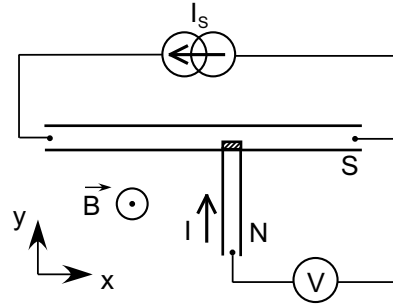


FIG. 1: Layout of the experiment: a 10  $\mu\text{m}$ -long, 120 nm-wide and 40 nm-thick superconducting (aluminum) wire can be current biased at  $I_S$  or exposed to a magnetic field  $B$ . A normal probe electrode forms a tunnel junction (dashed area) with the wire. To a good approximation (see text), the differential conductance of the junction  $dI/dV(V)$  is proportional to the DOS in the superconductor.

The 10  $\mu\text{m}$ -long aluminum wire, with width  $w = 120$  nm and thickness  $t = 40$  nm, was superficially oxidized in order to form a tunnel barrier with the copper probe electrode overlapping it on an area  $150 \times 60$  nm<sup>2</sup>. The sample was mounted in a copper box thermally anchored to the mixing chamber of a dilution refrigerator. Measurements were performed at 25 mK. Electrical connections were made through filtered coaxial lines. From the low-temperature, high-magnetic-field wire resistance in the normal state,  $R = 77$   $\Omega$ , the conductivity  $\sigma = 27$   $\Omega^{-1} \cdot \mu\text{m}^{-1}$  is inferred assuming that the electrical cross-section of the wire is  $S = wt$ . The diffusion coefficient  $D = 49$  cm<sup>2</sup>·s<sup>-1</sup> is then deduced using Einstein's relation  $\sigma = N(0)e^2D$ , where  $N(0) = 2.15 \cdot 10^{47}$  J<sup>-1</sup>·m<sup>-3</sup> is the density of states at the Fermi level of aluminum in its normal state and  $e$  the electronic charge. The superconducting gap  $\Delta_0 = 205$   $\mu\text{eV}$  was deduced from the differential conductance-voltage characteristic  $dI/dV(V)$  measured at  $B = 0$ ,  $I_s = 0$  (dashed line in Fig. 2). Using these parameters, we obtain the superconducting coherence length  $\xi_0 = \sqrt{\hbar D/\Delta_0} \approx 125$  nm and the London length  $\lambda_L = \sqrt{\hbar/(\mu_0\pi\sigma\Delta_0)} \approx 175$  nm. Since  $\lambda_L \gg w/2$ , the current density is homogeneous when the wire is current-biased, and a magnetic field penetrates uniformly in the wire. The measured critical current of the wire at  $B = 0$  was  $I_c = 106$   $\mu\text{A}$ .

In Fig. 2, two  $dI/dV(V)$  curves are shown, respectively measured at  $I_s = 70$   $\mu\text{A}$ , zero field, and at zero current,  $B = 23$  mT. The reduction of the gap and the smearing of the peak near the gap energy are similar in the two situations, bringing already evidence of the equivalent effect of  $I_s$  and  $B$ . Note that the magnetic

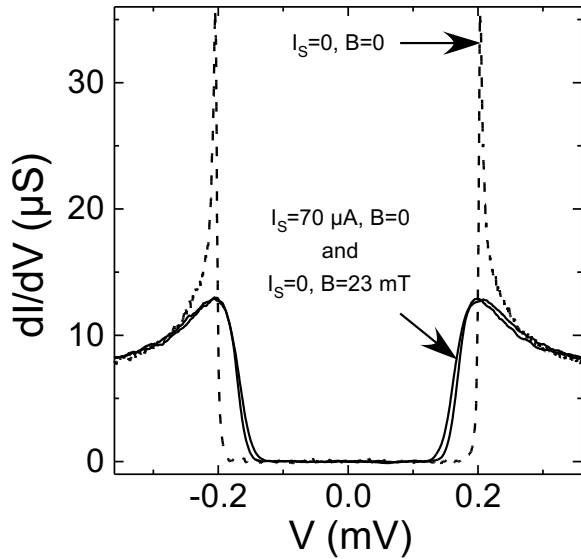


FIG. 2: Measured  $dI/dV(V)$  for different combinations of the bias current and magnetic field: dashed line:  $I_s = 0$  and  $B = 0$ ; solid lines:  $I_s = 70$   $\mu\text{A}$  and  $B = 0$ , and  $I_s = 0$  and  $B = 23$  mT.

field created by the supercurrent has a negligible effect: for  $I_s = 70$   $\mu\text{A}$  in the wire (see Fig. 2),  $\frac{\mu_0 I_s}{2\pi w} \sim 0.15$  mT whereas the resulting DOS is recovered at  $I_s = 0$  with  $B = 23$  mT. A complete set of data is presented in Fig. 3, with  $dI/dV(V)$  measured for  $I_s = 17, 51$  and  $85$   $\mu\text{A}$  at  $B = 0$ , and for  $B = 11.5$  to  $69$  mT by steps of  $11.5$  mT, at  $I_s = 0$ . Note that when the wire is current biased, the superconducting state is metastable. In practice, for bias currents larger  $85$   $\mu\text{A}$ , the system switches to the resistive state during the recording of the  $dI/dV(V)$  curve. The measured curve is then similar to that obtained in the normal state. In order to account quantitatively for the data, we use the Usadel theory [3, 4]. In this theory, correlations between electrons of opposite spins and momenta are described by a complex function  $\theta(\vec{r}, E)$ , the pairing angle, which depends both on space and energy, and a local complex phase  $\varphi(\vec{r}, E)$ . The local density of states is given by  $n(\vec{r}, E) = N(0)\text{Re}[\cos(\theta(\vec{r}, E))]$ . The pairing angle and the complex phase obey the Usadel equations:

$$\frac{\hbar D}{2} \nabla^2 \theta + [iE - \frac{\hbar D}{2} (\vec{\nabla} \varphi - \frac{2e}{\hbar} \vec{A})^2 \cos \theta] \sin \theta + \Delta \cos \theta = 0 \quad (1)$$

$$\vec{\nabla} [(\vec{\nabla} \varphi - \frac{2e}{\hbar} \vec{A}) \sin^2 \theta] = 0. \quad (2)$$

A term describing spin-flip scattering, which is found negligible in our experiment, has been omitted here. The pairing potential  $\Delta(\vec{r})$  is determined self-consistently by

$$\Delta(\vec{r}) = N(0)V_{eff} \int_0^{\hbar\omega_D} dE \tanh(\frac{E}{2k_B T}) \text{Im}(\sin \theta) \quad (3)$$

where  $V_{eff}$  is the pairing interaction strength,  $\omega_D$  the Debye pulsation,  $k_B$  the Boltzmann constant and  $T$  the temperature of the superconductor.

The supercurrent density  $\vec{j}$  is given by:

$$\vec{j}(\vec{r}) = \frac{\sigma}{e} \int_0^{\infty} dE \tanh(\frac{E}{2k_B T}) \text{Im}(\sin^2 \theta) (\vec{\nabla} \varphi - \frac{2e}{\hbar} \vec{A}). \quad (4)$$

In a situation like ours where the system consists entirely of a single superconductor,  $\vec{\nabla} \varphi$  does not depend on energy, and  $\vec{j}$  can be written as a product of the density of charge in the superconducting state  $\rho_S(\vec{r}) = eN(0)U_S(\vec{r})$ , with  $U_S(\vec{r}) = \int_0^{\infty} dE \tanh(\frac{E}{2k_B T}) \text{Im}(\sin^2 \theta)$ , and of a superfluid velocity  $\vec{v}_S = D(\vec{\nabla} \varphi - (2e/\hbar)\vec{A})$ .

We have first checked numerically that the dependence of  $\theta$  on the directions transverse to the wire could be neglected because the width and thickness are smaller than the superconducting coherence length  $\xi_0$ , which is the characteristic lengthscale for the variations of  $\theta$ . As a consequence, all the quantities can be replaced by their values averaged on the transverse directions. In the London gauge, the effect of the magnetic field is described

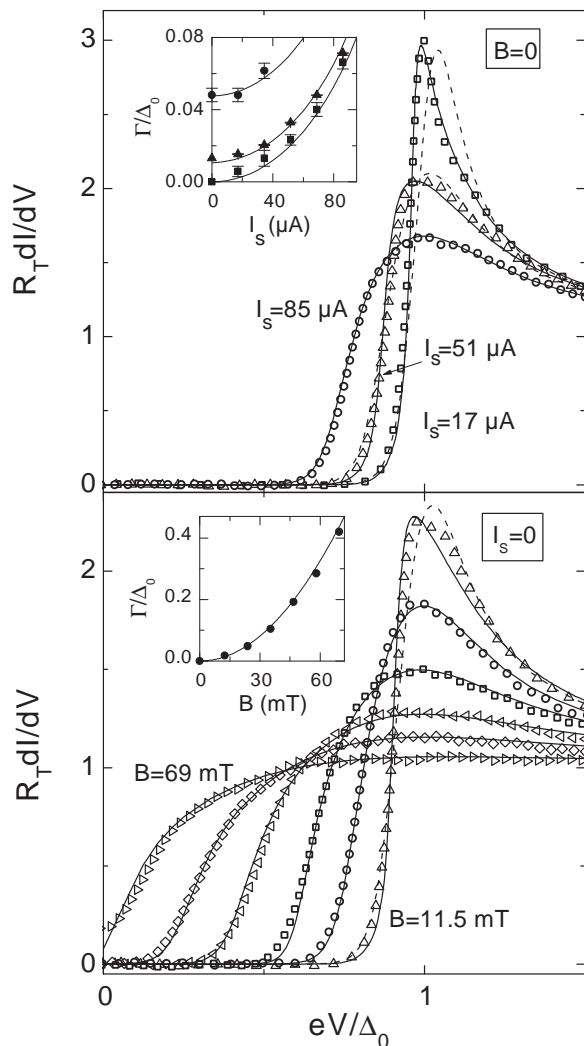


FIG. 3: Normalized differential conductance  $dI/dV(V)$  of the probe tunnel junction: Top: at  $B = 0$ , as a function of the supercurrent  $I_S$  (from right to left:  $I_S = 17 \mu\text{A}$ ,  $51 \mu\text{A}$ , and  $85 \mu\text{A}$ ). Bottom: at  $I_S = 0$ , as a function of the magnetic field  $B$  (from 11.5 mT to 69 mT by steps of 11.5 mT). Solid lines are best fits with  $dI/dV(V)$  calculated with an electronic temperature dependent on  $V$  (see text); dashed lines are the best fits with  $dI/dV(V)$  calculated with a constant electronic temperature. Insets: depairing energy  $\Gamma$  (in units of the gap  $\Delta_0$ ) at  $B = 0$  and  $I_S = 0$  for different currents and magnetic fields, deduced from the fits of  $dI/dV(V)$ . In the top inset, square symbols correspond to the data in the main panel ( $B = 0$ ), whereas triangles and disks were obtained from data taken at  $B = 10.2$  mT and  $B = 27$  mT, respectively. Solid lines: Fits with theory, leading to depairing current and magnetic field  $I_\Gamma = 240 \mu\text{A}$  and  $B_\Gamma = 105$  mT.

by a vector potential parallel to the wire axis  $x$ , with an amplitude  $A_x = By$ , so that  $\langle A_x \rangle = 0$  and  $\sqrt{\langle A_x^2 \rangle} = Bw/(2\sqrt{3})$  [11]. The constant phase gradient  $\partial\varphi/\partial x$  is given by the supercurrent  $I_S = jS = U_S L / (eR) (\partial\varphi/\partial x)$ . Since  $\partial^2\varphi/\partial x^2 = 0$ , Eq. (2) reduces to  $\partial(\sin^2\theta)/\partial x = 0$ . No spatial dependence remains in Eq. (1), and one re-

covers the generic equation given in Ref. [2]:

$$E + i\Gamma \cos\theta = i\Delta \frac{\cos\theta}{\sin\theta} \quad (5)$$

where

$$\Gamma = \frac{\hbar D}{2} \left( \left( \frac{\partial\varphi}{\partial x} \right)^2 + \left( \frac{2e}{\hbar} \right)^2 \langle A_x^2 \rangle \right) \quad (6)$$

is the depairing energy, which contains the effect of both a phase gradient and a magnetic field. Note that since  $\Gamma/\Delta_0 = \frac{1}{2}(\xi_0\partial\varphi/\partial x)^2 + \frac{1}{6}(\xi_0 w B / (\hbar/e))^2$  the relevant parameters are the phase difference between two points of the wire distant by  $\xi_0$  and the number of flux quanta in an area  $w\xi_0$ . The depairing energy is related to the external parameters  $I_S$  and  $B$  by the equation:

$$\frac{\Gamma}{\Delta_0} = \left( \frac{\Delta_0}{U_S(\Gamma)} \frac{I_S}{I_\Gamma} \right)^2 + \left( \frac{B}{B_\Gamma} \right)^2, \quad (7)$$

where we have introduced the characteristic depairing current and magnetic field  $I_\Gamma = \sqrt{2}\Delta_0/(eR(\xi_0))$ , with  $R(\xi_0) = R\xi_0/L$  the resistance of the wire on a length  $\xi_0$ , and  $B_\Gamma = \sqrt{6}(\hbar/e)/(w\xi_0)$ . Since the transverse dimensions of the wire are smaller than the London length  $\lambda_L$ , the depairing energy due to the induced field is negligible (smaller by a factor  $\sim 10^{-4}$  [12]) compared to the one due to the supercurrent. The DOS for a given depairing energy  $\Gamma$  is obtained from the self-consistent solution of Eqs. (3) and (5). For practical purposes, we give the approximate expressions for the resulting  $\Delta(\Gamma)/\Delta_0$  and  $U_S(\Gamma)/\Delta_0$ , valid, at  $k_B T \ll \Delta$ , for  $\Gamma/\Delta_0 \lesssim 0.3$ :

$$\frac{\Delta(\Gamma)}{\Delta_0} \simeq 1 - 0.75 \frac{\Gamma}{\Delta_0} - 0.54 \left( \frac{\Gamma}{\Delta_0} \right)^2 \quad (8)$$

$$\frac{U_S(\Gamma)}{\Delta_0} \simeq \pi/2 - 1.8 \frac{\Gamma}{\Delta_0} - 1.0 \left( \frac{\Gamma}{\Delta_0} \right)^2.$$

The differential conductance measured in the experiments is not exactly proportional to the density of states  $n(E)$  in the superconducting wire. Two effects must be taken into account in order to calculate  $dI/dV(V)$  from  $n(E)$ : Coulomb blockade and the temperature of the probe electrode. Coulomb blockade results from the finite impedance of the electromagnetic environment of the tunnel junction [5]. The characteristics of the environment are found from the  $dI/dV(V)$  characteristic of the circuit in the normal state, reached at  $B > 0.1$  T, which presents a 10% logarithmic dip at zero voltage. The environment can be modeled by a capacitance  $C = 8$  fF in parallel with a resistance  $R = 250 \Omega$ . Coulomb blockade results in a convolution of the density of states with a function  $P(E)$ , the probability for the electromagnetic environment of the tunnel junction to absorb an energy  $E$  [13]:

$$\frac{dI}{dV}(V) = \frac{1}{R_t} \int_0^{eV} dE n(E) P(eV - E). \quad (9)$$

Here,  $P(E) = \alpha/E_0(E/E_0)^{\alpha-1}$  for  $E$  smaller than  $E_0 = e^2/\pi\alpha C$ , with  $\alpha = 2R/(h/e^2)$ . The tunnel resistance of the junction was  $R_t = 140$  k $\Omega$ . As a result of this correction, the peak value of  $n(E)$  is reduced by a few % in  $dI/dV(V)$ . Finite temperature in the normal probe results in a further convolution with the derivative of a Fermi function. In our experimental setup, this temperature is slightly voltage-dependent, because the probe electrode is thermally isolated from the larger contact pads by superconducting connections. Heat transport only occurs by electron-phonon coupling and by electron tunneling through the junction. Since both mechanisms are very inefficient, even an input power  $\mathcal{P}_{\text{in}}$  in the fW range can induce a significant temperature increase. At bias voltages large compared to the superconducting gap, heating by the tunneling current has a sizeable effect. In contrast, at bias voltages  $V$  slightly below  $\Delta/e$ , only quasiparticles at energies larger than  $\Delta - eV$  can tunnel, resulting in evaporative cooling [14]. The effective electron temperature  $T$  is obtained by solving the heat equation:

$$\Sigma\Omega(T^5 - T_{ph}^5) - \mathcal{P}_{\text{in}} + \int dE \frac{E}{e^2 R_T} n(E+eV)(1-f(E)) = 0. \quad (10)$$

The first term describes heat transfer to the phonon bath, with  $\Sigma \simeq 2$  nW. $\mu\text{m}^{-3}$ .K $^{-5}$  for Cu [10],  $\Omega \simeq 0.08$   $\mu\text{m}^3$  the volume of the normal region of the probe electrode, and  $T_{ph} = 25$  mK the phonon temperature. The second term accounts for additional uncontrolled heat flow, that we attribute to spurious electromagnetic noise. The third term accounts for heat transfer through the junction, with  $f(E)$  the Fermi function at temperature  $T$ . From the fit of the data at  $B = 0$  and  $I_s = 0$ , we find  $\mathcal{P}_{\text{in}} = 185$  aW, corresponding to  $T = 65$  mK at  $eV \ll \Delta_0$ . The maximum cooling effect is reached at  $eV/\Delta_0 = 0.99$ , where  $T = 30$  mK; heating dominates for  $eV/\Delta_0 > 1.02$ , with  $T = 210$  mK at  $eV/\Delta_0 = 1.5$ .

In Fig. 3, we present with solid lines best fits of the data, taking into account both Coulomb blockade and temperature corrections. The values of the fit parameter  $\Gamma$  for each curve are given in the insets. For a comparison, are also shown with dashed lines fits with a constant electron temperature ( $T = 60$  mK). The  $V$ -dependent temperature correction only matters for the sharpest curves. In turn, by fitting  $\Gamma(I_s, B)/\Delta_0$  with Eq. (7) and (8), we find  $I_\Gamma = 240$   $\mu\text{A}$  and  $B_\Gamma = 105$  mT. The theoretical values, assuming that the electrical dimensions of the wire are identical to the geometrical ones, are  $I_\Gamma = 310$   $\mu\text{A}$  and  $B_\Gamma = 105$  mT. Conversely, the experimental values of  $I_\Gamma \propto \xi_0^{-1}$  and  $B_\Gamma \propto (w\xi_0)^{-1}$  can be used to extract effective values  $\xi_{0\text{eff}} = 162$  nm (instead of 125 nm) and  $w_{\text{eff}} = 93$  nm (instead of 120 nm). This corresponds in turn to an increased value of the diffusive coefficient:  $D = 81$  cm $^2$ s $^{-1}$  and, through the resistance, to an effective thickness  $t_{\text{eff}} = 31$  nm (instead of 40 nm). Reduced

effective dimensions for electrical transport could be attributed partly to the surface oxidation of the aluminum, which was exposed to air at atmospheric pressure before measurement, and to surface roughness.

A by-product of the Usadel equations is a straightforward calculation of the critical current. According to Eq. (4),  $I_s \propto U_s(\Gamma)\partial\varphi/\partial x$ . Since  $U_s(\Gamma)$  decreases with  $\Gamma$ ,  $I_s$  presents a maximum as a function of  $\partial\varphi/\partial x$ , which is the thermodynamic critical current. At  $B = 0$  and  $k_B T \ll \Delta_0$ , the maximum occurs at  $\xi_0\partial\varphi/\partial x \approx 0.69$ , and corresponds, in agreement with [15], to  $I_c \approx 0.75S\Delta_0^{3/2}\sqrt{N(0)\sigma/\hbar} \approx 0.53I_\Gamma = 125$   $\mu\text{A}$  (using the experimental determination of  $I_\Gamma$ ). The difference with the measured  $I_c = 106$   $\mu\text{A}$  might be due to the uncontrolled environment of the wire and to inhomogeneities in the wire cross-section.

In conclusion, we have measured by tunneling spectroscopy on a superconducting wire the effect on the superconducting order of a supercurrent  $I_s$  and of an external magnetic field  $B$ . As predicted by the theory of superconductivity in diffusive conductors, the overall effect solely depends on a single parameter, the depairing energy  $\Gamma$ . For our narrow wire, the Usadel equations lead to a simple expression for this depairing energy as a function of  $I_s$  and  $B$ , which compares well with the experimental determination of  $\Gamma$ .

We thank C. Mitescu for the communication of his PhD thesis and for correspondance, and N. Birge for his comments on the manuscript. We acknowledge the technical help of P. Orfila, and permanent input from M. Devoret, P. Joyez, F. Pierre, C. Urbina, and D. Vion.

- 
- [1] J. Bardeen, L. N. Cooper, and J. R. Schrieffer, Phys. Rev. **108**, 1175 (1957).
  - [2] For a review, see K. Maki in *Superconductivity*, edited by R.D. Parks (Marcel Dekker, New York, 1969), p. 1035.
  - [3] K.D. Usadel, Phys. Rev. Lett. **25**, 507 (1970).
  - [4] For a review, see W. Belzig, F. Wilhelm, C. Bruder, G. Schön and A.D. Zaikin, Superlattices and Microstructures, vol. **25** No 5/6 (1999) (cond-mat/9812297).
  - [5] S. Gueron, H. Pothier, N. O. Birge, D. Esteve and M.H. Devoret, Phys. Rev. Lett. **77**, 3025 (1996).
  - [6] B. Pannetier and H. Courtois, J. Low Temp. Phys. **188**, 599 (2000); H. Courtois, P. Charlat, Ph. Gandit, D. Mailly and B. Pannetier, J. Low Temp. Phys. **116**, 187 (1999); P. Dubos, H. Courtois, B. Pannetier, F. K. Wilhelm, A.D. Zaikin, and G. Schoen, Phys. Rev. B **63**, 064502 (2001).
  - [7] J.L. Levine, Phys. Rev. **155**, 373 (1967). In this work, the films were thick enough to ensure that the depairing effect was dominating the Zeeman effect.
  - [8] C. D. Mitescu, PhD thesis, California Institute of Technology, Pasadena (1966).
  - [9] M. Tinkham, *Introduction to Superconductivity* (Mc Graw Hill, 1985).
  - [10] F. Pierre, Ann. Phys. (Paris) **26** N4 (2001).

- [11] When taking into account the screening of the magnetic field inside the superconductor, we get a negligible correcting factor  $\approx 1 - 1/60(w/\lambda_L)^2 \approx 0.99$ .
- [12] For a cylindrical wire with cross-area  $S$ , the ratio is  $(S/\lambda_L^2)^2/90$ .
- [13] For a review, see G.-L. Ingold and Yu. Nazarov, in *Single Charge Tunneling*, Ed. H. Grabert and M. H. Devoret (Plenum Press, New York, 1992).
- [14] M. Nahum, T.M. Eiles, J.M. Martinis, Appl. Phys. Lett. **65**, 3123 (1994).
- [15] J. Romijn, T.M. Klapwijk, M.J. Renne, and J.E. Mooij, Phys. Rev. B **26**, 3648 (1982).